

1           **Identifying deep moonquake nests using machine**  
2           **learning model on single lunar station on the far side of**  
3           **the Moon**

4           **Josipa Majstorović<sup>1</sup>, Philippe Lognonné<sup>1</sup>, Taichi Kawamura<sup>1</sup>, Mark P.**  
5           **Panning<sup>2</sup>**

6           <sup>1</sup>Université Paris Cité, Institut de physique du globe de Paris, CNRS, Paris, France  
7           <sup>2</sup>Jet Propulsion Laboratory, California Institute of Technology, Pasadena, CA, USA

8           **Key Points:**

- 9           • As a part of the future space mission NASA will deploy a new seismic station to  
10           Schrödinger Basin on the far side of the Moon.  
11           • We propose a machine learning model trained to classify deep moonquakes using  
12           the lunar orbital parameter.  
13           • The models perform with accuracy greater than 70% when trained to classify com-  
14           binations of four or fewer nests.

---

Corresponding author: Josipa Majstorović, [josipa.majstorovic@protonmail.com](mailto:josipa.majstorovic@protonmail.com)

**Abstract**

One of the future NASA space program includes the Farside Seismic Suite (FSS) payload, a single station with two seismometers, on the far side of the Moon. During FSS operations, the processing of the data will provide us with new insight into the Moon's seismic activity. One of Apollo mission finding is the existence of deep moonquakes (DMQ), and the nature of their temporal occurrence patterns as well as the spatially clustering. It has been shown that DMQs reside in about 300 source regions. In this paper we tackle how we can associate new events with these source regions using the single station data. We propose a machine learning model that is trained to differentiate between DMQ nests using only the lunar orbital parameters related to DMQ time occurrences. We show that ML models perform well (with an accuracy  $> 70\%$ ) when they are trained to classify less than 4 nests.

**Plain Language Summary**

The future space missions will provide us with various new lunar data, one of which will be ground vibration measurement. The studies of these measurements from the Apollo era in 70s, showed that Moon can host various events. The most intriguing ones are deep moonquakes (DMQs), which are events associated with the displacement deep within the lunar interior. It has been shown that DMQs occur in the specific locations, which are called nests, and that their temporal occurrence is related to the monthly motion of the Moon around the Earth. In this paper we tackle how we can associate new events from only one station located on the far side of the Moon with these known locations of DMQs. We propose a machine learning model that is trained to classify DMQ nests, only using the information about their temporal occurrences, e.g. time of the event, described in terms of different lunar events. We report that models are performing well (with an accuracy  $> 70\%$ ) when they are trained to classify 4 or fewer nests. This gives us a good first approximation about the nest identification.

**1 Introduction**

We are at the beginning of a golden age of lunar exploration as many nations, together with private companies, are establishing numerous efforts to obtain new scientific measurement of the Moon (Weber et al., 2021; Pickrell, 2022; Kawamura et al., 2022). In light of this, NASA established the Artemis program which should land a crewed mission at the lunar south pole (Witze, 2022). This would be the first attempt of a crewed landing after the successful Apollo missions in 1970's. Before Artemis missions land on the Moon, NASA has also established the Commercial Lunar Payload Services (CLPS) program to land scientific payloads on the Moon using commercial landers. The Farside Seismic Suite (FSS) is one of the selected payloads, and it will deliver two seismometers to Schrödinger Basin on the far side of the Moon (Panning et al., 2021; Standley et al., 2023; Cutler et al., 2023): one vertical Very BroadBand seismometer, and Short Period sensor, both spare or derived from the SEIS experiment sensors (Lognonné et al., 2019, 2020) from the InSight mission to Mars (Banerdt et al., 2020).

The Apollo missions showed the importance of deploying sensors on the surface of the Moon, since a great deal of our knowledge about the Moon comes from the analysis of data acquired during the Apollo era (Lognonné & Johnson, 2015). Thus, analyzing ground motion measurements provided the community with the first constraints on the lunar interior and the activity at the surface (Nakamura et al., 1982a, 1982b; Khan et al., 2000; Khan & Mosegaard, 2002; Khan et al., 2014; Lognonné et al., 2003; Gagnepain-Beyneix et al., 2006; Weber et al., 2010; Garcia et al., 2011; Kawamura et al., 2017; Garcia et al., 2019; Nunn et al., 2020). It has also revealed that the Moon can host events of various origins, such as shallow and deep moonquakes, meteoroid and artificial impacts (Toksöz et al., 1974; Dainty et al., 1975; Lammlein, 1977a; Nakamura, 1983, 2003, 2005).

65 Today, we have more than twelve thousands events, out of which the deep moonquakes  
66 (DMQs) form the most numerous group (Nakamura et al., 1981; Nakamura, 2005).

67 DMQs are a distinctive group of seismic events that originate from depths between  
68 700 and 1200 km, at high pressure and temperature conditions, where little brittle de-  
69 formation is expected. Due to very high waveform similarity between quakes, the DMQs  
70 have been clustered into about 300 source regions or nests (Nakamura, 2003). This has  
71 interpreted to be a consequence of DMQs occurring repeatedly at the fixed nests, which  
72 are located mostly on the near side of the Moon. It has been shown that time occurrence  
73 of the DMQs is correlated with the monthly motion of the Moon around the Earth. Thus,  
74 DMQ occurrences exhibit tidal periodicities and furthermore, the associated high strain  
75 rates might explain brittle processes (Kawamura et al., 2017). However, the real causes  
76 of their origins are yet to be discovered. There are two puzzling fact about their origin:  
77 a) cyclic tidal stresses, caused by the monthly motion of Moon around Earth, are far less  
78 than the estimated confining pressures where DMQs occurs (Cheng & Toksöz, 1978; Min-  
79 shull & Gouly, 1988a); b) do we need both, tectonic and ambient tidal stresses, to ex-  
80 plain their mechanical origin (Frohlich & Nakamura, 2009).

81 To better constrain the lunar interior and unravel the cause of DMQs, it is impor-  
82 tant to locate new events and associate them with the known nest locations from Apollo  
83 with future lunar missions like FSS. These new observations will add, for each new nest,  
84 a new differential  $t_s - t_p$  measurement constraining the deep interior with a different  
85 epicentral distance. However, due to the mission requirements, it is extremely likely that,  
86 at the beginning, we might have only one lunar station at the disposal. Therefore, in this  
87 paper we study the problem of DMQ nest identification without using waveform infor-  
88 mation. This is due to the new location of the recording station, which will not match  
89 existing Apollo-era waveform templates due to different propagation paths. We propose  
90 a machine learning (ML) model that is trained to identify nests within the set of nests  
91 of similar differential travel times. The main features used for the model training are re-  
92 lated to the fact that different nests respond differently to lunar cycle.

93 Very early studies have shown correlation between lunar transient events and po-  
94 sition of the Moon related to the Earth (Middlehurst, 1967; Cameron & Gilheany, 1967;  
95 Moore, 1968). This further encouraged observations that some moonquakes occur with  
96 periods that reflect Earth-Moon-Sun relationship (Ewing et al., 1971). Later, it has been  
97 shown that the occurrence of DMQs are related to tidal stress cycles, and correlations  
98 between DMQs occurrence times and lunar monthly tidal cycles have been indicated (Lammlein  
99 et al., 1974; Toksöz et al., 1977; Lammlein, 1977b; Cheng & Toksöz, 1978; Minshull &  
100 Gouly, 1988b). The lunar cycle can be explained with three lunar months: synodic, dra-  
101 conic, anomalistic. Synodic month is the period of lunar phases such as New Moon, First  
102 Quarter, Full Moon, Last Quarter. Draconic month is the period between two nodes, as-  
103 cending or descending, where the nodes are points at which the Moon's orbit plane crosses  
104 the ecliptic plane towards which it is inclined of about  $5.14^\circ$ . Anomalistic month is the  
105 period between two extreme points, perigee and apogee, since the Moon's orbit approx-  
106 imates an ellipse rather than a circle. Earlier studies counted the number of events per  
107 day as a function of time and found 0.5 and 1 month signals in the occurrence times re-  
108 lated to anomalistic and draconic period of 27 days (Lammlein et al., 1974; Lammlein,  
109 1977b). The same studies also indicated 206-day and 6-year periods, related to the Sun's  
110 perturbation on the lunar orbit and the relative precession of the perigee of the Moon's  
111 orbit. Subsequently, many recent papers studied and confirmed tidal periodicities of DMQs  
112 and more (Bulow et al., 2005, 2007; Bills et al., 2008; Frohlich & Nakamura, 2009; We-  
113 ber et al., 2009, 2010; Turner et al., 2022).

114 Based on the previous papers, it is clear that DMQ nests exhibit some clear tem-  
115 poral patterns in their occurrences, and that these are correlated with Moon-Earth sys-  
116 tem. Therefore, the open question is whether we can design features which would reflect  
117 these temporal patterns and to further use those features to study the nest identifica-

118 tion with one lunar station. In this paper we tackle the question of defining optimal fea-  
 119 tures and the machine learning model. The paper is organised as follows: first, we dis-  
 120 cuss data used in the analysis, the existing catalog of DMQ events. Second, we discuss  
 121 the feature design. Third, we introduce a machine learning model. Fourth, we discuss  
 122 successes and pitfalls of the machine learning model for nest identification applied to dif-  
 123 ferent combination of nests. We conclude how this study can offer some first estimates  
 124 of the nest location in the future lunar missions.

## 125 2 Data

126 We start with the existing catalog of lunar events (Nakamura et al., 1981), which  
 127 was updated in 2008 and modified in 2018 (Nunn et al., 2020). Catalog contains a list  
 128 of events (shallow and deep moonquakes, meteoroid and artificial impacts) with attributes  
 129 such as date and time of the event occurrence, signal envelope amplitude as measured  
 130 in mm on a standard plot, data availability per station, and the nest (source) classifi-  
 131 cation for DMQs. It is important to note that the source classification is not an exact  
 132 location defined by latitude and longitude, rather a result from the waveform cross-correlation  
 133 and single-link cluster analysis (Nakamura, 2003). This analysis positively clustered around  
 134 7k DMQs into 77 nests, where the largest nest is associated with label A1. This nest con-  
 135 tains 443 quakes and it is placed on the near side of the Moon.

### 136 2.1 Catalog processing: nest sets based on travel time information

137 Earlier studies published lunar interior models and location of DMQ nests in terms  
 138 of latitude and longitude by picking P and S travel times on the quake waveforms (Garcia  
 139 et al., 2019, review of these picks). Using lunar interior models and nest locations we can  
 140 define nests that are close by in distance if we consider only the  $t_{sp}$  travel time measure-  
 141 ments. To do so we assume that a) our single lunar station is located on the far side in  
 142 Schrödinger Basin (FSS landing site at  $71.378^\circ\text{S}$ ,  $138.248^\circ\text{E}$ ), b) nests' latitudes and lon-  
 143 gitudes from (Lognonné et al., 2003), c) calculated P- and S- wave travel times ( $t_p$  and  
 144  $t_s$ , respectively) using lunar velocity model between landing site and locations of DMQ  
 145 nests. By having  $t_s$  and  $t_p$  we can calculate  $t_{sp} = t_s - t_p$  for all nests and models shown  
 146 in Figure 1 (see Text S1 and Figure S1 for further explanation). Next, we count for each  
 147 nest how many there are with the similar  $t_{sp}$  travel time measurement assuming a pick-  
 148 ing error of 5 seconds as shown in Figure 1A, consistent with the average picking error  
 149 in Lognonné et al. (2003). This count provides us with the different sets  $S_i$ , shown in  
 150 Figure 1A, that contain nests  $N_j$  of similar travel times. In other words, if we are able  
 151 to measure  $t_s$  and  $t_p$  of the new lunar event with accuracy within 5 seconds, we are not  
 152 able to differentiate between nests that belong to different sets  $S_i$ . Therefore, to further  
 153 tackle the nest identification problem we proceed to associate each event with a com-  
 154 bination of lunar orbital measurements.

### 155 2.2 Feature selection based on the lunar orbital information

156 It has been shown that the DMQ temporal patterns in time occurrences are related  
 157 to different lunar cycles and that these patterns differ from nest to nest. Three lunar cy-  
 158 cles are synodic, draconic, anomalistic, and they all have similar periods, but are marked  
 159 by different motions, either as the motion between two Full Moons phases, or two nodes,  
 160 or two apsis, respectively. One can list all the events when Moon is in the Full Moon (New  
 161 Moon) phase, passing through ascending (descending) node or perigee (apogee) by sim-  
 162 ply looking at the Moon's ephemeris (Meeus, 1991). To make sure that we take into ac-  
 163 count the temporal patterns, we design the main three features as a time difference be-  
 164 tween the time of the quake in the nest and the time of the Moon's Full Moon, ascend-  
 165 ing node and perigee, denoting it as  $\Delta t_{FullMoon}$ ,  $\Delta t_{AscendingNode}$ ,  $\Delta t_{Perigee}$ , respectively.  
 166 We can achieve the same effect by taking the other three time axis as referent one (New

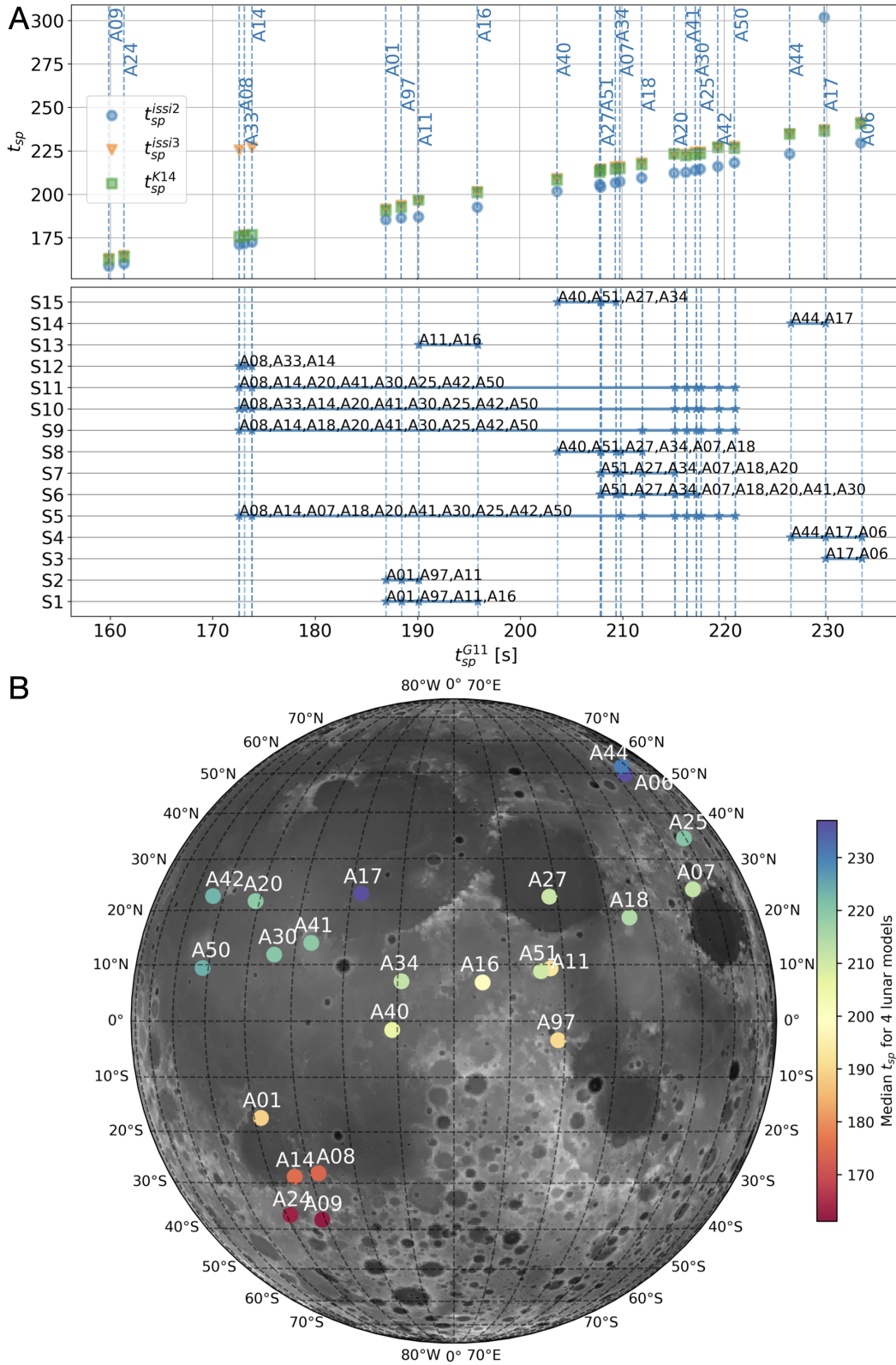


**Figure 1.** Location study of the DMQ nests from the perspective of  $t_{sp} = t_s - t_p$  travel time measurements if we place station in the Schrödinger Basin and consider four different lunar models. A) Upper panel:  $t_{sp}$  travel time measurements for four lunar models from Garcia et al. (2011) (G11), Garcia et al. (2019) (issi2, issi3), (Khan et al., 2014) (K14) with nest labels; A) Lower panel: Sets  $S_i$  which represent nests with similar travel times if we consider a travel time error of 5 seconds. B) Lunar map with the nests locations where the color indicate the median  $t_{sp}$  for four lunar model.

167 Moon, descending node, and apogee). The next feature is related to the Moon position  
 168 within its orbit as in Frohlich and Nakamura (2009). The angle between the direction  
 169 of perigee and the current position of the body, as seen from the main focus of the el-  
 170 lipse, is called the true anomaly, denoted further as  $\gamma$ . Further, as one of the feature we  
 171 also use the interval time between two quakes in the nest, noted as  $e_{i+1}-e_i$ , as in Weber  
 172 et al. (2010). And the last two features are related to the position of the Moon with re-  
 173 spect to the Earth, and these are the distance,  $d$ , itself and the rate of the distance change,  
 174  $\dot{d}$ , as in Bills et al. (2008).

175 The selected features all have different ranges and we refer to them as raw data.  
 176 To train a model that is able to generalise well for a given problem sometimes it is nec-  
 177 essary to transform raw data to a form that is more suitable for training (Langer et al.,  
 178 2019). By applying transformation on the raw data we may obtain a mapping which bet-  
 179 ter reveals patterns in our data. Therefore, we chose to apply trigonometric transforma-  
 180 tion of the true anomaly angle  $\gamma$ , to properly address the jump discontinuities in the fea-  
 181 ture when angle goes from  $2\pi$  to 0, due to its cyclic nature. This is addressed by trans-  
 182 forming true anomaly angle  $\gamma$  to pair of  $[\cos \gamma, \sin \gamma]$ . An example of all eight features  
 183 are shown in Figure S2 for nest A1.

### 184 3 Methodology

185 When new lunar data arrives, we shall be able to differentiate events in groups based  
 186 on the waveform similarity measurement. And we shall be able to measure their P and  
 187 S travel times, and thus form set of nests from Section 2.1. Final step would be to as-  
 188 sociate these new events with the existing Apollo nests if possible. This nest identifica-  
 189 tion from a single lunar station is a supervised classification problem. The model is trained  
 190 in a predictive way by taking into account nest locations as labels and nest lunar orbital  
 191 parameters as input data. Since we want to predict a class (nest), but we do not have  
 192 statistically large data set (as previously mentioned A1 has 443 quakes), we choose to  
 193 train a Random Forest (RF) Classifier, since RF can perform well with any size of datasets  
 194 and tend not to overfit (Ho, 1995; Breiman, 2001).

195 Random Forest (RF) is a machine learning technique that is based on decision trees  
 196 (Breiman et al., 1984; Quinlan, 1986) and bootstrap aggregating (Breiman, 1996), where  
 197 the main output is reached by majority votes among an ensemble of randomised deci-  
 198 sion trees. A main building unit, a decision tree, is a tree-like learning algorithm where  
 199 each internal node tests on attribute, each branch corresponds to attribute value and each  
 200 leaf node represents the final prediction. Usually, during the training phase thresholds,  
 201 order and number of inequality operations within internal nodes are learned. The hy-  
 202 perparameters that define a RF structure, such as the number of trees, and measure which  
 203 maximises diversity between classes, are determined beforehand (see Text S2 and Fig-  
 204 ure S3).

205 RF also provides an assessment of the feature or input variable importance which  
 206 might give us an insight of how the model reached its prediction. To assess the feature  
 207 importance, the RF removes one of the features while it keeps the rest constant, and it  
 208 measures, among others, the accuracy decrease (Breiman, 2001). RF models are able to  
 209 solve regression and classification problems, as well as two- and multi-class problems. It  
 210 has been show that RF can perform with high accuracy even though there are only a  
 211 few parameters to tune.

212 In our case, during the training phase, the RF model has access to the extracted  
 213 features of the individual quakes and the nest labels. The training is performed on a sub-  
 214 set of the data, while the model performance is evaluated on the test subset, which the  
 215 model has never seen. Evaluation is accomplished by comparing the model's predicted  
 216 class (nest) with the ground truth one. The statistical performance of the model is pre-

217 sented with confusion matrix and Receiver Operating Characteristic (ROC) curve. We  
 218 expect that in the case of the ideal RF Classifier the diagonal of the confusion matrix is  
 219 equal to 1 (and off-diagonal elements are zero), while ROC curve is passing through the  
 220 left upper corner.

## 221 4 Results and discussion

### 222 4.1 Training and testing on two largest nests

223 We first test the hypothesis whether it is possible to differentiate two DMQ nests  
 224 using the lunar orbital parameters (features). For this, we select the two largest nests,  
 225 A1 and A8, with a total size of 768 events and ratio A1:A8=0.57 : 0.43 (see feature dis-  
 226 tributions in Figure S4).

227 Training and testing our base RF model (see Text S2) with the normalised and not  
 228 normalised input data, we end up selecting to work with the normalised input data since  
 229 this model performed better (see Figure S5 and S6). The base model trained with the  
 230 normalised input data performed with an accuracy of 89%, while precision, recall and  
 231 f1-score for the A1 nest is 88%, 94%, 91%, respectively, and for A8 is 90%, 80%, 85%,  
 232 respectively (see Figure S6B) with only the occurrence time knowledge. The ROC curve  
 233 is above the random classifier curve, meaning that the base model is not randomly clas-  
 234 sifying A1 and A8 nests (see Figure S6C). Out of eight features, the first five most im-  
 235 portant are  $\cos(\gamma)$ ,  $\Delta t_{Perigee}$ ,  $d$ ,  $\Delta t_{AscendingNode}$ ,  $e_{i+1} - e_i$  (see Figure S6D). We no-  
 236 tice that  $\cos(\gamma)$  is the feature with the most important contribution to the model learn-  
 237 ing. This might be because A1 and A8 have reversed distributions for  $\cos(\gamma)$  feature (see  
 238 Figure S 4D).

239 We proceed into testing learning robustness of our base model in a series of exper-  
 240 iments (see Text S2 and Figures S7-S12), all of which indicate that the model is stable.  
 241 This implies that the base model generalizes well, and not over fit the results. Further,  
 242 if we examine why the base model sometimes mislabels the nests (Figure S13), we no-  
 243 tice that the 2D manifold (see Text S3) of feature space spanned by the input data, cal-  
 244 culated by t-sne method (van der Maaten & Hinton, 2008), is not perfectly separated.  
 245 It seems this segregation might be dominated by a single feature, and that is  $\Delta t_{AscendingNode}$   
 246 (see Figure S14 and S15A).

### 247 4.2 Training and testing on three and more nests

248 In this section we study how the performance of our base RF model from Section  
 249 4.1 changes by adding more nests. We carry out three tests for the next combinations  
 250 and their ratios: A1-A8-A18 (45%-33%-22%), A1-A8-A18-A6 (38%-28%-18%-15%), A1-  
 251 A8-A18-A6-A14 (33%-25%-16%-13%-12%), where the three added nests are the three  
 252 largest nests besides A1 and A8.

253 The analysis shows that by adding more nests, the performance of our base model  
 254 deteriorates since the accuracy drops from 88% to 59% (see Figures S16-S19). By adding  
 255 a 3rd nest, and we notice that A1 and A8 recalls deteriorate slightly, and 50% is A18 events  
 256 are classified either as A1 or A8 (see Figure S16). Yet, the precision of A18 is the high-  
 257 est. Features,  $e_{i+1} - e_i$  and  $d$ , gain importance. Yet, the importance of all features be-  
 258 come more equalized. By adding a 4th nest, A6, the recall of A1 nest improves, recall  
 259 of A8 nest deteriorates even more than before, recall of A18 improves notably, and the  
 260 new added nest A6 has a recall of 46%, by having most of its events misclassified only  
 261 as A1 nest, and not a single event as A18 (see Figure S17). This might implies that A18  
 262 and A6 nests have completely different source mechanisms. Less notably than before,  
 263 the importance of all features is becoming more equalized. Lastly, by adding a 5th nest,  
 264 A14, the recall of A1 and A8 become the highest, and three other nests perform with

265 recall less than 50%, and their most mislabelled data points are associated with A1 nest  
 266 (see Figure S18). The importance between features is almost equalized, yet the inter-  
 267 val time  $e_{i+1} - e_i$  is the only feature that stands out.

268 These results might imply that by adding more nests, we add more complexity into  
 269 the problem, since we might be adding nests that have similar source mechanisms. Hav-  
 270 ing similar source mechanisms means that sources are triggered by tides is the same way,  
 271 so their lunar orbital features have similar characteristics, and we cannot differentiate  
 272 between nests without having more data. Furthermore, it seems that the only signifi-  
 273 cantly important feature is the interval time, the only feature that does not reflect the  
 274 lunar orbital information.

275 Checking the two dimensional representation of the feature space constructed by  
 276 the feature combination of nests A1-A8-A18-A6-A14, we might conclude that for this  
 277 particular set it is to some degree impossible to completely differentiate between nests  
 278 due to the lack of data (see Figure S20).

### 279 4.3 Training and testing on nest sets

280 Using the same base RF model from Section 4.1, we proceed to train and test how  
 281 well we can differentiate nests that belong to the same set shown in Figure 1. We an-  
 282alyze them in three separate groups by the frequency of the nest they contain: A) S1,  
 283 S2, S3, S4, S12, S13, S14, S15; B) S5, S6, S7, S8; C) S9, S10, S11. The results are shown  
 284 in Figure 2A, B, and C, respectively.

285 We observe high value of recall for most of the nests, as well as high accuracy for  
 286 most of the sets (see Figure 2). Sets that have  $\leq 4$  nests perform better than those with  
 287 more nests, as in sets from group A shown in Figure 2B. When the nest's recall is very  
 288 low or zero (A11, A30, A41, A42, A50), it signifies a nest with very few events (see ra-  
 289tio of nests in all sets in Figure S18). If we take an example of nest A20, we notice that  
 290 it has constant recall in many sets (see Figure 2B and C), even though it is not the biggest  
 291 nest in the set (see Figure S21). Thus, not only the size but probably also the unique-  
 292ness of the features determine the success of identifying the nest.

293 The importance of different features is shown in Figure 3 for all three groups. On  
 294 one hand, removing just one nest could change the feature importance, as in the case  
 295 of S2 (where we remove A16) versus S1. On the other hand, we notice that the feature  
 296 importance does not drastically change when comparing results for sets S3 and S4, where  
 297 we add nest A44, even though the nest itself is large in size (see Figure S21). For the sets  
 298 in group B, the feature importance is stable with respect to adding or removing nests.  
 299 It is quite similar for group C, where only one set S8 has different feature importance.  
 300 We notice that sets which contain  $\leq 4$  nests (as in group A), there is usually one or  
 301 two important features, while for sets with  $> 4$  nests there is equalisation of the feature  
 302 importance (as in groups B and C). This might imply that a single lunar orbital param-  
 303eter is enough to explain the occurrence of the nests, which are unique in nature. Mix-  
 304ing more nests suggests that we might be mixing nests with similar temporal patterns,  
 305 thus learning how to differentiate them is more challenging. Moreover, the feature im-  
 306portance changes for sets that have unique combinations of nests, which may hint that  
 307 these nests have different source mechanisms.

308 If we consider a 2D manifold spanned by the sets from groups A, B, C (see Fig-  
 309ures S22, S23, S24, respectively), we notice that unique segregation in this space corre-  
 310lates with the RF model accuracy. Nests that form closely spaced homogenized clusters  
 311 in the 2D manifold tend to be correlated with models that scored high recall for these  
 312 nests.

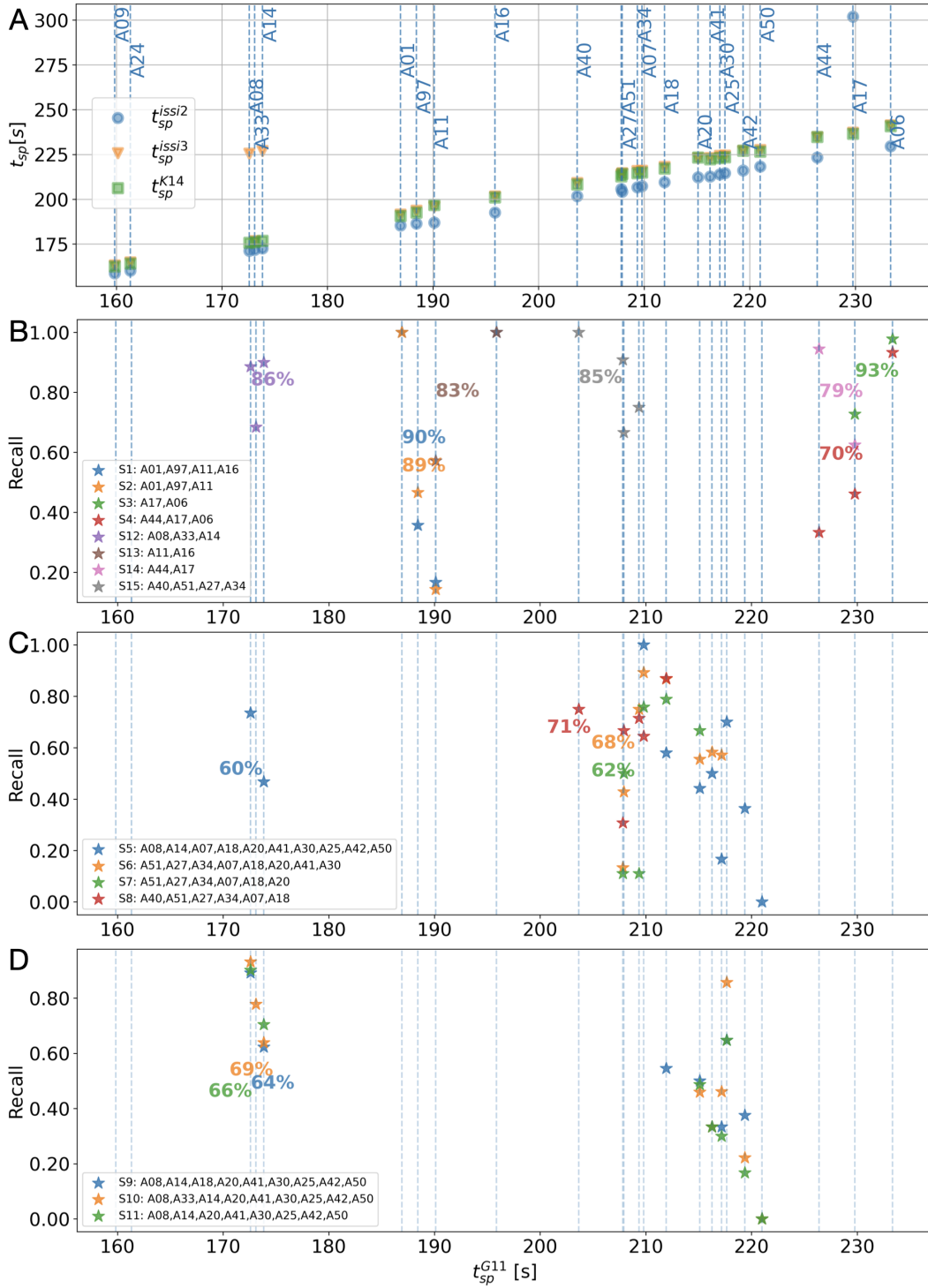


**Figure 2.** Performance of RF models designed to classify nests within different sets. A) Travel times  $t_{sp}$  for four lunar model from Garcia et al. (2011) (G11), Garcia et al. (2019) (issi2, issi3), (Khan et al., 2014) (K14) with nest labels. B) Recall for individual nests within each set with respect to their travel times labeled with sets to which they belong and the scored accuracy of this set. C) and D) same as B) just for different group of sets.

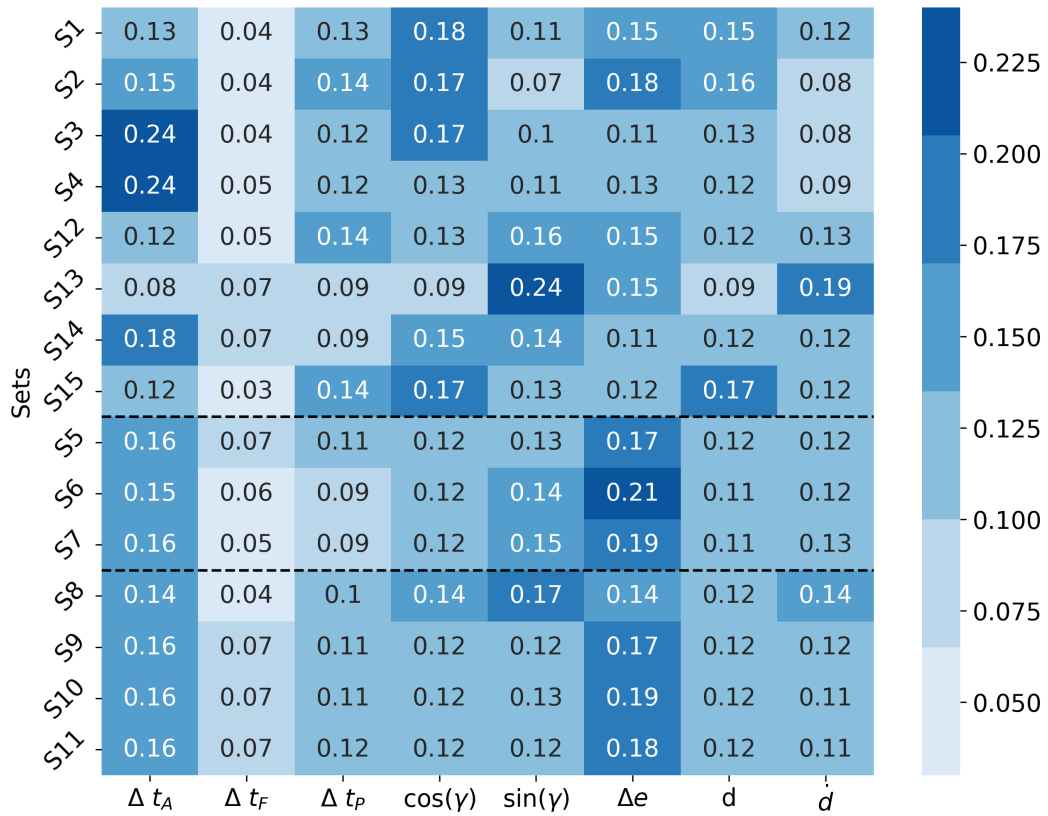


**Figure 3.** Feature importance for Random Forest models associated with different travel time sets shown in Figure 1.

## 5 Conclusion

In this paper we propose how to tackle DMQ nest identification during future lunar missions that will likely host only one station on the far side of the Moon. We propose constraining their location by using differential time travel measurement  $t_{sp}$  and parameters related to the temporal patterns of the DMQ occurrence. First, in our analysis we assume that we cannot differentiate between nests whose differences in travel time are less than 5 seconds. Thus, we form set of nests that have similar travel times. Second, for each event within the nests we calculate features that are used to build a Random Forest model. This model is trained to differentiate between distinct nests. The features used for training are build by associating each event in all nests with the time difference between events' origin time and time of lunar ascending node, Full Moon phase, perigee, then position of the Moon in its orbit expressed by true anomaly angle, distance of the Moon from the Earth, rate change of this distance, and the time between two successive quakes. We show that by training Random Forest models to differentiate between distinct nests within sets, we can obtain models with high accuracy (more than half of the models score above 70% accuracy). Yet, the performances of these models depend on the number of nests within the set. More nests implies that the problem is more difficult to solve, probably because a) nests might have similar source mechanisms, b) the number of events within nests is unbalanced, and c) we don't have enough data. Since RF models also arrange features by their importance to make a final classification decision, we observe that the importance of the features change with different sets. This complements the findings of previous papers, since it signifies that nests do correspond to different lunar events, which eventually might be connected to the distribution of tidal stresses during these events. Finally, our model provides a good first approximation of the nest identification. And as the catalog of new events grows, it will be straightforward to retrain RF model with the new enlarged dataset.

## Open Research Section

The deep moonquake catalog used in this study is published in Nakamura et al. (1981), and revisited in Nunn et al. (2020). Python package Skyfield used to calculate Moon's orbital parameters based on JPL ephemeris can be found on the website <https://rhodesmill.org/skyfield/> (Rhodes, 2019, Software). For our implementation of the Random Forest algorithm we use Scikit-learn machine learning Python library (Pedregosa et al., 2011).

## Acknowledgments

French co-authors thanks the French Space Agency, CNES, for supporting this research in the frame of the French contribution to FSS as well as IDEX Paris Cité (ANR-18-IDEX-0001). MPP was supported by funds from the Jet Propulsion Laboratory, under contract with the National Aeronautics and Space Administration (NASA).

## References

- Banerdt, W. B., Smrekar, S. E., Banfield, D., Giardini, D., Golombek, M., Johnson, C. L., ... others (2020). Initial results from the insight mission on mars. *Nature Geoscience*, *13*(3), 183–189.
- Bills, B. G., Bulow, R., & Johnson, C. L. (2008). Influence of earth-moon orbit geometry on deep moonquake occurrence times. *Lunar Planet. Sci.*, *XXXIX*.
- Breiman, L. (1996). Bagging predictors. *Machine learning*, *24*, 123–140.
- Breiman, L. (2001). Random forests. *Machine learning*, *45*, 5–32.
- Breiman, L., Friedman, J., Stone, C. J., & Olshen, R. A. (1984). *Classification and regression trees*. CRC press.

- 361 Bulow, R., Johnson, C., Bills, B., & Shearer, P. (2007). Temporal and spatial prop-  
 362 erties of some deep moonquake clusters. *Journal of Geophysical Research:*  
 363 *Planets*, 112(E9).
- 364 Bulow, R., Johnson, C., & Shearer, P. (2005). New events discovered in the apollo  
 365 lunar seismic data. *Journal of Geophysical Research: Planets*, 110(E10).
- 366 Cameron, W. S., & Gilheany, J. J. (1967). Operation moon blink and report of ob-  
 367 servations of lunar transient phenomena. *Icarus*, 7(1-3), 29–41.
- 368 Cheng, C. H., & Toksöz, M. N. (1978). Tidal stresses in the moon. *Journal of*  
 369 *Geophysical Research: Solid Earth*, 83(B2), 845–853. Retrieved from [https://](https://agupubs.onlinelibrary.wiley.com/doi/abs/10.1029/JB083iB02p00845)  
 370 [agupubs.onlinelibrary.wiley.com/doi/abs/10.1029/JB083iB02p00845](https://agupubs.onlinelibrary.wiley.com/doi/abs/10.1029/JB083iB02p00845)  
 371 doi: <https://doi.org/10.1029/JB083iB02p00845>
- 372 Cutler, J. W., Nguyen, T. A., Kano, T., Kumar, Y. R. L., Panning, M., April, S., &  
 373 Haque, S. (2023). Overview of the avionics design for the farside seismic suite.  
 374 In *Aiaa scitech 2023 forum*. Retrieved from [https://arc.aiaa.org/doi/abs/](https://arc.aiaa.org/doi/abs/10.2514/6.2023-1880)  
 375 [10.2514/6.2023-1880](https://arc.aiaa.org/doi/abs/10.2514/6.2023-1880) doi: 10.2514/6.2023-1880
- 376 Dainty, A., Goins, N., & Toksoz, M. (1975). Natural lunar seismic events and the  
 377 structure of the moon. In *In: Lunar science conference, 6th, houston, tex.,*  
 378 *march 17-21, 1975, proceedings. volume 3.(a78-46741 21-91) new york, perga-*  
 379 *mon press, inc., 1975, p. 2887-2897.* (Vol. 6, pp. 2887–2897).
- 380 Ewing, M., Latham, G., Press, F., Sutton, G., Dorman, J., Nakamura, Y., ... Ko-  
 381 vach, R. (1971). Seismology of the moon and implications on internal struc-  
 382 ture, origin and evolution. *Highlights of astronomy*, 2, 155–172.
- 383 Frohlich, C., & Nakamura, Y. (2009). The physical mechanisms of deep moon-  
 384 quakes and intermediate-depth earthquakes: How similar and how differ-  
 385 ent? *Physics of the Earth and Planetary Interiors*, 173(3), 365–374. Re-  
 386 trieved from [https://www.sciencedirect.com/science/article/pii/](https://www.sciencedirect.com/science/article/pii/S0031920109000338)  
 387 [S0031920109000338](https://www.sciencedirect.com/science/article/pii/S0031920109000338) doi: <https://doi.org/10.1016/j.pepi.2009.02.004>
- 388 Gagnepain-Beyneix, J., Lognonné, P., Chenet, H., Lombardi, D., & Spohn, T.  
 389 (2006). A seismic model of the lunar mantle and constraints on tempera-  
 390 ture and mineralogy. *Physics of the Earth and Planetary Interiors*, 159(3-4),  
 391 140–166.
- 392 Garcia, R. F., Gagnepain-Beyneix, J., Chevrot, S., & Lognonné, P. (2011). Very pre-  
 393 liminary reference moon model. *Physics of the Earth and Planetary Interiors*,  
 394 188(1-2), 96–113.
- 395 Garcia, R. F., Khan, A., Drilleau, M., Margerin, L., Kawamura, T., Sun, D., ... oth-  
 396 ers (2019). Lunar seismology: An update on interior structure models. *Space*  
 397 *Science Reviews*, 215, 1–47.
- 398 Ho, T. K. (1995). Random decision forests. In *Proceedings of 3rd international con-*  
 399 *ference on document analysis and recognition* (Vol. 1, pp. 278–282).
- 400 Kawamura, T., Grott, M., Garcia, R., Wiczorek, M., de Raucourt, S., Lognonné,  
 401 P., ... others (2022). An autonomous lunar geophysical experiment package  
 402 (algep) for future space missions: In response to call for white papers for the  
 403 voyage 2050 long-term plan in the esa science program. *Experimental Astron-*  
 404 *omy*, 54(2-3), 617–640.
- 405 Kawamura, T., Lognonné, P., Nishikawa, Y., & Tanaka, S. (2017). Evaluation of  
 406 deep moonquake source parameters: Implication for fault characteristics and  
 407 thermal state. *Journal of Geophysical Research: Planets*, 122(7), 1487–1504.
- 408 Khan, A., Connolly, J. A. D., Pommier, A., & Noir, J. (2014). Geophysical evi-  
 409 dence for melt in the deep lunar interior and implications for lunar evolution.  
 410 *Journal of Geophysical Research: Planets*, 119(10), 2197–2221. Retrieved  
 411 from [https://agupubs.onlinelibrary.wiley.com/doi/abs/10.1002/](https://agupubs.onlinelibrary.wiley.com/doi/abs/10.1002/2014JE004661)  
 412 [2014JE004661](https://agupubs.onlinelibrary.wiley.com/doi/abs/10.1002/2014JE004661) doi: <https://doi.org/10.1002/2014JE004661>
- 413 Khan, A., & Mosegaard, K. (2002). An inquiry into the lunar interior: A nonlin-  
 414 ear inversion of the apollo lunar seismic data. *Journal of Geophysical Research:*  
 415 *Planets*, 107(E6), 3–1.

- 416 Khan, A., Mosegaard, K., & Rasmussen, K. L. (2000). A new seismic velocity model  
417 for the moon from a monte carlo inversion of the apollo lunar seismic data.  
418 *Geophysical Research Letters*, *27*(11), 1591–1594.
- 419 Lammlein, D. R. (1977a). Lunar seismicity and tectonics. *Physics of the*  
420 *Earth and Planetary Interiors*, *14*(3), 224–273. Retrieved from [https://](https://www.sciencedirect.com/science/article/pii/0031920177901753)  
421 [www.sciencedirect.com/science/article/pii/0031920177901753](https://www.sciencedirect.com/science/article/pii/0031920177901753) doi:  
422 [https://doi.org/10.1016/0031-9201\(77\)90175-3](https://doi.org/10.1016/0031-9201(77)90175-3)
- 423 Lammlein, D. R. (1977b). Lunar seismicity and tectonics. *Physics of the Earth and*  
424 *Planetary Interiors*, *14*(3), 224–273.
- 425 Lammlein, D. R., Latham, G. V., Dorman, J., Nakamura, Y., & Ewing, M. (1974).  
426 Lunar seismicity, structure, and tectonics. *Reviews of Geophysics*, *12*(1), 1–21.
- 427 Langer, H., Falsaperla, S., & Hammer, C. (2019). *Advantages and pitfalls of pattern*  
428 *recognition: selected cases in geophysics*. Elsevier.
- 429 Lognonné, P., Banerdt, W. B., Giardini, D., Pike, W. T., Christensen, U., Laudet,  
430 P., ... others (2019). Seis: Insight’s seismic experiment for internal structure  
431 of mars. *Space Science Reviews*, *215*, 1–170.
- 432 Lognonné, P., Banerdt, W. B., Pike, W. T., Giardini, D., Christensen, U., Garcia,  
433 R. F., ... others (2020). Constraints on the shallow elastic and anelastic struc-  
434 ture of mars from insight seismic data. *Nature Geoscience*, *13*(3), 213–220.
- 435 Lognonné, P., Gagnepain-Beyneix, J., & Chenet, H. (2003). A new seismic model of  
436 the moon: implications for structure, thermal evolution and formation of the  
437 moon. *Earth and Planetary Science Letters*, *211*(1-2), 27–44.
- 438 Lognonné, P., & Johnson, C. (2015). 10.03—planetary seismology. *Treatise on geo-*  
439 *physics*, *2*, 65–120.
- 440 Meeus, J. (1991). Astronomical algorithms. *Richmond*.
- 441 Middlehurst, B. M. (1967). An analysis of lunar events. *Reviews of Geophysics*,  
442 *5*(2), 173–189.
- 443 Minshull, T., & Gouly, N. (1988a). The influence of tidal stresses on deep moon-  
444 quake activity. *Physics of the Earth and Planetary Interiors*, *52*(1), 41–55.  
445 Retrieved from [https://www.sciencedirect.com/science/article/pii/](https://www.sciencedirect.com/science/article/pii/0031920188900568)  
446 [0031920188900568](https://www.sciencedirect.com/science/article/pii/0031920188900568) doi: [https://doi.org/10.1016/0031-9201\(88\)90056-8](https://doi.org/10.1016/0031-9201(88)90056-8)
- 447 Minshull, T., & Gouly, N. (1988b). The influence of tidal stresses on deep moon-  
448 quake activity. *Physics of the earth and planetary interiors*, *52*(1-2), 41–55.
- 449 Moore, P. (1968). Transient lunar phenomena: A review, 1967. *J. Br. Astron. As-*  
450 *soc.*, *78*, 138–144.
- 451 Nakamura, Y. (1983). Seismic velocity structure of the lunar mantle. *Journal of*  
452 *Geophysical Research: Solid Earth*, *88*(B1), 677–686. Retrieved from [https://](https://agupubs.onlinelibrary.wiley.com/doi/abs/10.1029/JB088iB01p00677)  
453 [agupubs.onlinelibrary.wiley.com/doi/abs/10.1029/JB088iB01p00677](https://agupubs.onlinelibrary.wiley.com/doi/abs/10.1029/JB088iB01p00677)  
454 doi: <https://doi.org/10.1029/JB088iB01p00677>
- 455 Nakamura, Y. (2003). New identification of deep moonquakes in the apollo lunar  
456 seismic data. *Physics of the Earth and Planetary Interiors*, *139*(3), 197–205.  
457 Retrieved from [https://www.sciencedirect.com/science/article/pii/](https://www.sciencedirect.com/science/article/pii/S0031920103002103)  
458 [S0031920103002103](https://www.sciencedirect.com/science/article/pii/S0031920103002103) doi: <https://doi.org/10.1016/j.pepi.2003.07.017>
- 459 Nakamura, Y. (2005). Farside deep moonquakes and deep interior of the moon.  
460 *Journal of Geophysical Research: Planets*, *110*(E1). Retrieved from [https://](https://agupubs.onlinelibrary.wiley.com/doi/abs/10.1029/2004JE002332)  
461 [agupubs.onlinelibrary.wiley.com/doi/abs/10.1029/2004JE002332](https://agupubs.onlinelibrary.wiley.com/doi/abs/10.1029/2004JE002332) doi:  
462 <https://doi.org/10.1029/2004JE002332>
- 463 Nakamura, Y., Latham, G., Dorman, H., & Harris, J. (1981). Passive seismic ex-  
464 periment long-period event catalog. *Galveston Geophysics Laboratory Contribu-*  
465 *tion*, *491*, 314.
- 466 Nakamura, Y., Latham, G. V., & Dorman, H. J. (1982a). Apollo lunar seismic  
467 experiment—final summary. *Journal of Geophysical Research: Solid Earth*,  
468 *87*(S01), A117–A123.
- 469 Nakamura, Y., Latham, G. V., & Dorman, H. J. (1982b). Apollo lunar seismic  
470 experiment—final summary. *Journal of Geophysical Research: Solid Earth*,

- 471 87(S01), A117-A123. Retrieved from <https://agupubs.onlinelibrary>  
 472 [.wiley.com/doi/abs/10.1029/JB087iS01p0A117](https://doi.org/10.1029/JB087iS01p0A117) doi: [https://doi.org/](https://doi.org/10.1029/JB087iS01p0A117)  
 473 [10.1029/JB087iS01p0A117](https://doi.org/10.1029/JB087iS01p0A117)
- 474 Nunn, C., Garcia, R. F., Nakamura, Y., Marusiak, A. G., Kawamura, T., Sun, D.,  
 475 ... others (2020). Lunar seismology: A data and instrumentation review.  
 476 *Space Science Reviews*, 216(5), 89.
- 477 Panning, M., Kedar, S., Bowles, N., Calcutt, S., Cutler, J., Elliott, J., ... others  
 478 (2021). Farside seismic suite (fss): First seismic data from the farside of the  
 479 moon delivered by a commercial lander. In *Agu fall meeting abstracts* (Vol.  
 480 2021, pp. P54C–01).
- 481 Pedregosa, F., Varoquaux, G., Gramfort, A., Michel, V., Thirion, B., Grisel, O.,  
 482 ... others (2011). Scikit-learn: Machine learning in python. *the Journal of*  
 483 *machine Learning research*, 12, 2825–2830.
- 484 Pickrell, J. (2022, May). These six countries are about to go to the moon — here’s  
 485 why. *Nature*, 605, 208–211. doi: 10.1038/d41586-022-01252-7
- 486 Quinlan, J. R. (1986). Induction of decision trees. *Machine learning*, 1, 81–106.
- 487 Rhodes, B. (2019). Skyfield: Generate high precision research-grade positions for  
 488 stars, planets, moons, and earth satellites. *Astrophysics Source Code Library*,  
 489 ascl-1907.
- 490 Standley, I. M., Pike, W. T., Calcutt, S., & Hoffman, J. P. (2023). Short period seis-  
 491 mometer for the lunar farside seismic suite mission. In *2023 ieee aerospace con-*  
 492 *ference* (p. 1-9). doi: 10.1109/AERO55745.2023.10115559
- 493 Toksöz, M. N., Dainty, A. M., Solomon, S. C., & Anderson, K. R. (1974). Structure  
 494 of the moon. *Reviews of Geophysics*, 12(4), 539-567. Retrieved from [https://](https://agupubs.onlinelibrary.wiley.com/doi/abs/10.1029/RG012i004p00539)  
 495 [agupubs.onlinelibrary.wiley.com/doi/abs/10.1029/RG012i004p00539](https://agupubs.onlinelibrary.wiley.com/doi/abs/10.1029/RG012i004p00539)  
 496 doi: <https://doi.org/10.1029/RG012i004p00539>
- 497 Toksöz, M. N., Goins, N. R., & Cheng, C. (1977). Moonquakes: Mechanisms and re-  
 498 lation to tidal stresses. *Science*, 196(4293), 979–981.
- 499 Turner, A. R., Hawthorne, J. C., & Gaddes, M. (2022). Stresses in the lunar  
 500 interior: Insights from slip directions in the a01 deep moonquake nest. *Jour-*  
 501 *nal of Geophysical Research: Planets*, 127(12), e2022JE007364. Retrieved  
 502 from [https://agupubs.onlinelibrary.wiley.com/doi/abs/10.1029/](https://agupubs.onlinelibrary.wiley.com/doi/abs/10.1029/2022JE007364)  
 503 [2022JE007364](https://doi.org/10.1029/2022JE007364) doi: <https://doi.org/10.1029/2022JE007364>
- 504 van der Maaten, L., & Hinton, G. (2008). Visualizing data using t-sne. *Journal*  
 505 *of Machine Learning Research*, 9(86), 2579–2605. Retrieved from [http://jmlr](http://jmlr.org/papers/v9/vandermaaten08a.html)  
 506 [.org/papers/v9/vandermaaten08a.html](http://jmlr.org/papers/v9/vandermaaten08a.html)
- 507 Weber, R., Bills, B., & Johnson, C. (2009). Constraints on deep moonquake focal  
 508 mechanisms through analyses of tidal stress. *Journal of Geophysical Research:*  
 509 *Planets*, 114(E5).
- 510 Weber, R., Bills, B., & Johnson, C. (2010). A simple physical model for deep moon-  
 511 quake occurrence times. *Physics of the Earth and Planetary Interiors*, 182(3-  
 512 4), 152–160.
- 513 Weber, R., Neal, C., Grimm, R., Grott, M., Schmerr, N., Wiczorek, M., ... oth-  
 514 ers (2021). The scientific rationale for deployment of a long-lived geophysical  
 515 network on the moon. *Bulletin of the AAS*, 53(4).
- 516 Witze, A. (2022, May). The \$93-billion plan to put astronauts back on the moon.  
 517 *Nature*, 605, 212–216. doi: 10.1038/d41586-022-01253-6